

Modelling nutrient mass balance in a temperate meso-tidal estuary: Implications for management

João Magalhães Neto ^{a,*}, Mogens René Flindt ^b, João Carlos Marques ^a,
Miguel Ângelo Pardal ^a

^a IMAR – Institute of Marine Research (CIC), Department of Zoology, Faculty of Sciences and Technology,
Largo Marques de Pombal, University of Coimbra, 3004-517 Coimbra, Portugal

^b Institute of Biology, University of Southern Denmark, Campusvej 55, DK-5230 Odense M, Denmark

Received 20 October 2006; accepted 26 June 2007

Available online 8 August 2007

Abstract

Although mitigation programmes have been implemented in huge eutrophied estuarine systems, satisfactory results are not always immediately achieved. External loadings are reduced but the nutrient pools still existing in the sediments (due to decades of external supply) start to deplete only slowly, to reach the lower steady state level related to the new external loading. In the Mondego Estuary, this situation could be seen from the mass balance calculations including different nutrient fractions (dissolved, SPM and bound in vegetation). Different nutrient fractions quantified over the year showed the retention capacity and supplying capacity of these estuarine systems, and also the seasonal dynamics those fractions can present. External loading of nitrogen was largely dominated by DIN, but after its incorporation by benthic primary producers nitrogen export occurred essentially as SPM-N. Phosphorus loading was dominated by SPM-P, but during warmer periods P-efflux increased DIP concentration inside the system and was afterwards exported through the outer boundary. Although nutrients bound in vegetation were not significant to total mass balance, depending on the occurrence of occasional macroalgal blooms, the vegetation fraction can significantly increase its contribution to the overall balance.

A mathematical model was also created for the southern arm of the Mondego (MIKE 11), in the hope that it will become a reliable management tool that could help in future decisions relating to the system. The mass balance calculations and scenario analysis were based on nutrient field measurements and nutrient results from the hydrodynamic simulation (concentration of dissolved inorganic material, adsorbed to suspended particulate matter and bound in vegetation fractions). The importance of biological elements to estuarine dynamics was assessed, comparing simulations including these factors (water quality and eutrophication modules) with others containing only the hydrodynamic and advection–dispersion modules.

© 2007 Elsevier Ltd. All rights reserved.

Keywords: management; nutrient loading; transport; ecological modelling; mass balance; residence time

1. Introduction

Eutrophication of coastal waters as a result of anthropogenic activities is now widely recognised as a major pollution threat worldwide (Diaz and Rosenberg, 1995; Norkko and Bonsdorff, 1996; Valiela et al., 1997; Raffaelli et al., 1998;

Pardal et al., 2000, 2004; Sfriso et al., 2001). One of the main problems of these areas is the primary producer shift. Systems with low nutrient loadings are most often dominated by slow-growing vegetation (e.g. *Zostera* sp., *Fucus* sp.), while enhanced loading favours the growth of phytoplankton and opportunist macroalgae (e.g. *Ulva* sp.) as a secondary effect. Initially, changes occur in the actual nutrient dynamics and in the nutrient turnover, pushing the system to an unstable situation with respect to autotrophic and heterotrophic processes

* Corresponding author.

E-mail address: jneto@ci.uc.pt (J.M. Neto).

(Norkko and Bonsdorff, 1996; Raffaelli et al., 1998; Flindt et al., 1999; Martins et al., 2001; Sfriso et al., 2001; Cardoso et al., 2004). In the end, the loss of seagrass beds also leads to changes in the associated benthic community (Dolbeth et al., 2003; Cardoso et al., 2004), and to materials and services these areas are supposed to supply to their surroundings (Duarte, 2000; Jonge et al., 2000).

In the past few decades many management schemes have been implemented to reduce the external nutrient loading of coastal systems, which are now beginning to adjust to this decrease (Flindt et al., 1999; Kronvang et al., 1999; World Health Organization, 2002). To control the efficiency of mitigation measures for estuarine systems, monitoring programmes have been defined to check the loading, water quality and, in the end, the ecological status of the systems (e.g. under the Water Framework Directive – WFD).

Although the loading and the exporting of nutrients allow the estimation of the estuary's nutrient filtering/retention capacity (Mortazavi et al., 2000a,b; Nielsen et al., 2001) most of the nutrient mass balances calculated so far are incomplete. Traditionally, measurements were limited to dissolved inorganic nutrients and to nutrients adsorbed to fine particulate matter that could be trapped in filters (e.g. glass fibre filters). Others, such as the transported fraction bound to plants, were not included although they are essential for the nutrient mass balance of shallow productive micro- and meso-tidal estuaries (Flindt et al., 1997, 1999, 2004; Salomonsen et al., 1999).

For these productive systems the plant-bound nutrient transport may be the dominating form of nitrogen and phosphorus exports (Flindt et al., 1997, 2004; Salomonsen et al., 1999). Although the overall number of measurements is still low, it seems that the plant-bound nutrient transport is less essential to the nutrient mass balance in macro-tidal systems, where the turbidity is high (Lefevre, 1994; Hemminga et al., 1996; Bouchard and Lefevre, 2000) and the production is lower. It seems that the plant cover in the lower part of the European saltmarsh areas is small. The major plant biomass in these areas is growing at higher elevations, where the plants are less exposed to hydrodynamic forces. This way only a small amount of plants are likely to be transported (Beefink, 1977; Lefevre, 1994; Hobbs and Norton, 1996), and they make a considerable contribution to these systems' mass balance.

Moreover, this scenario can change dramatically if nutrient enrichment occurs. This situation usually results in spring macroalgal blooms, thus allowing the plant-bound nutrient transport to have a strong influence on the mass balance calculations. Even if annual estimations present smaller differences, the amount of nutrients mobilised seasonally by plants really can change all through the year.

In recent decades, the water discharged from farmland loaded the south arm of the Mondego Estuary. The nutrient enrichment combined with limited light at the bottom and low hydrodynamics favoured macroalgal blooms and suppressed the seagrass growth in the system (Marques et al., 1993; Flindt et al., 1999; Lillebø et al., 1999; Martins et al., 1999, 2001; Pardal et al., 2000, 2004; Cardoso et al., 2002, 2004; Dolbeth et al., 2003). Some experimental measures were implemented

in 1997, and a reduction of macroalgal blooms was later observed. Enriched water discharges were reduced and hydrodynamic circulation improves slightly; nevertheless, the system is still exporting accumulated nutrients to adjacent areas, meaning that an unbalanced situation may prevail for several years to come.

The aims of this work were to: (a) build and calibrate an ecological model of a meso-tidal system that could be useful for environmental management; (b) evaluate the mass balance of the Mondego's southern arm enriched system, exposed to considerable turbidity; and (c) evaluate and compare the role and dynamics of each nutrient form (dissolved inorganic nutrients, nutrients adsorbed to suspended particulate matter, nutrients in the traditional detritus and nutrients bound in macro-detritus and living plants).

2. Materials and methods

2.1. Study site

The Mondego River is located in central Portugal. Its estuary is 21-km long and it flows through the final part of the Lower Mondego Valley, a region that comprises around 150 km² of good agricultural land. The final part of the estuary has two contrasting arms, north and south, separated by a 6-km long alluvial plain, the Morradeira Island. The north arm is 8–12 m deep at high tide. It is the principal navigation channel and is where the commercial and fishing harbours are located. The south arm (SA) is shallower (2–4 m at high tide) and it is almost silted up in the upper zones (Bd3– Fig. 1), so the fresh water from the Mondego River flows mainly through the north arm.

The SA is a tide-dominated system (7-km long, 0.5-km wide and 2.57-km² in area) where up to 75% of its total surface becomes exposed to air at low tide. Around 10% of the intertidal area is covered by rooted vegetation (e.g. *Scirpus maritimus* L., *Spartina maritima* (Curtis) Fernald, 1916, *Zostera noltii* Hornem.), and 65% corresponds to bare muddy and sandy bottoms. It receives a small water input from the north arm when the tide is high (through a 1-m² section channel opened experimentally at the splitting point of the two arms), an irregular contribution from the Armazéns channel (Bd2– Fig. 1), and a considerable freshwater contribution from the Pranto River (Bd1– Fig. 1). The freshwater discharged by this small tributary is controlled by a sluice that is essentially regulated according to the water needs of rice fields of the Mondego Valley. The south arm rejoins the north arm 1 km before the sea (Bd4– Fig. 1).

2.2. Sampling programme

There were 41 field campaigns in the SA between January 2000 and January 2001. They covered full tidal cycles (12 h) with different tidal amplitudes, and were assessed in four places inside the system (Fig. 1, Table 1): (a) SA outer boundary (Bd4); (b) Armazéns channel, immediately upstream from the junction point with the SA (I); (c) Pranto River, immediately

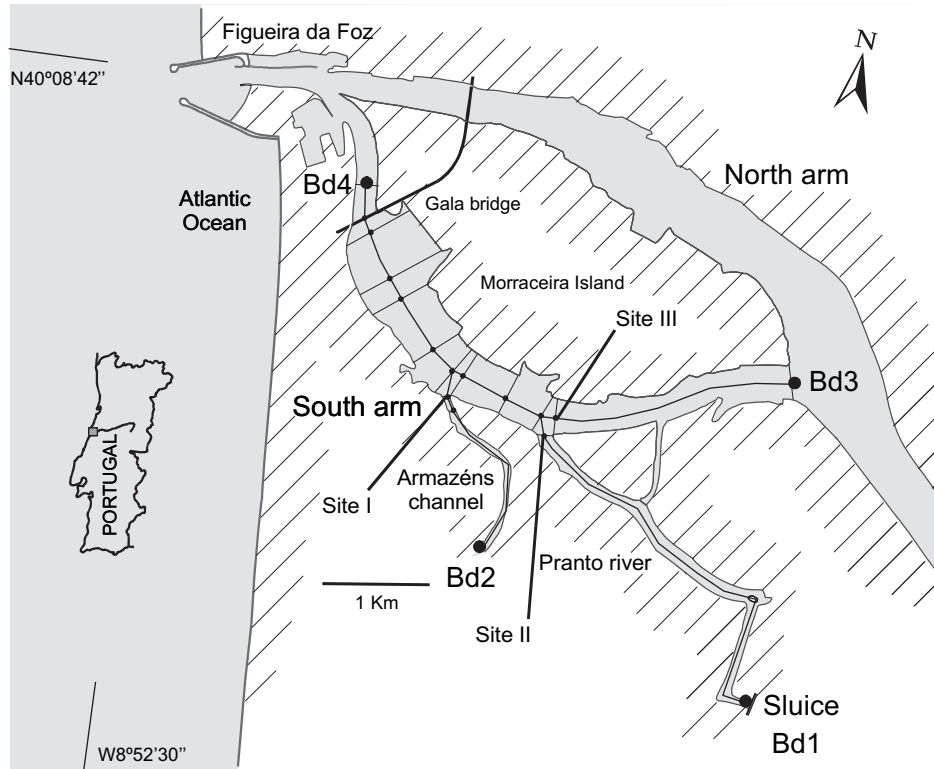


Fig. 1. Mondego River estuary: boundaries (Bd1 – sluice, Bd2 – Armazéns, Bd3 – south arm riverhead, Bd4 – outer boundary, in large circles), sampling sites (I, II and III) and cross-section profiles (small circles).

upstream from the junction point with the SA (II); and (d) at the SA riverhead, immediately upstream from where the Pranto River joins that channel (III). Measurements *in situ* were made every hour and included the water level, velocity, salinity, and the dissolved oxygen. Water samples were collected simultaneously for physico-chemical characterisation. Water samples were immediately filtered (pre-weighed Whatman GF/C glass fibre filters) and frozen until analysis. From each sample, one filter was folded and stored dehydrated until analysed for total nitrogen and total phosphorus in suspended particulate matter (SPM-N and SPM-P), and one other was used for chlorophyll *a* content analysis (APHA, 1980). Sub-samples of filters were analysed for SPM total C and N on a CHN analyser (Carlo Erba). The chlorophyll *a* analysis followed the techniques recommended by Strickland and Parsons (1972). At the sluice (Bd1) the water discharges were registered and their volumes evaluated by the water column section and velocity.

The drifting vegetation was collected using nets with an open metal frame of 0.5 × 0.5 m and 9 mm mesh size. The nets were placed on top of each other to cover the total height of the water column, and perpendicular to the water flow direction at representative locations inside the channel. Vegetation was sorted (macroalgae sheets, leaves, rhizomes, stems and roots) and weighed (g DW – 48 h, 70 °C and g AFDW – 8 h, 450 °C). Total N (Veg-N) and P (Veg-P) contents of different parts of plants were analysed according to Limnologisk Metodik (1992).

The calculation of vegetation export (biomass, N and P) was based on the proportion between green macroalgae export

and total vegetation export, and on the estimated relation between green macroalgae biomass drifted out (nets result) and present inside the system.

2.3. Model description (MIKE 11)

The MIKE 11 software (www.dhigroup.com) was used for the simulation work. It is a pseudo two-dimensional modelling tool with a computational scheme applicable to vertically homogeneous flow conditions that range from steep river flows to tide influenced estuaries. Its architecture is based on specific interacting sub-models that simulate the water motion, transport of substances in the water column, and the water quality and eutrophication conditions in the system (hydrodynamic – HD, advection–dispersion – AD, and water quality – WQ).

The hydrodynamic (HD) module solves the complete non-linear equations of open channel flow (Saint-Venant), vertically integrated equations for the continuity (conservation of mass) and momentum according to Eqs. (1) and (2):

$$\frac{\partial Q}{\partial x} + \frac{\partial A}{\partial t} = q \tag{1}$$

$$\frac{\partial Q}{\partial t} + \frac{\partial \left(\alpha \frac{Q^2}{A} \right)}{\partial x} + gA \frac{\partial h}{\partial x} + \frac{gQ|Q|}{M^2 AR^{4/3}} = 0 \tag{2}$$

where Q is the discharge ($\text{m}^3 \text{s}^{-1}$), A is the flow area (m^2), x is the distance (m), t is the time (s), q is the lateral inflow ($\text{m}^2 \text{s}^{-1}$), g is the acceleration due of gravity (m s^{-2}), h is

Table 1
Sampling sites and tidal amplitude over the study period

Date	Sampling site	Tidal amplitude (m)
29-01-2000	Bd4	1.1
19-03-2000	I	3.0
21-03-2000	Bd4	3.0
23-03-2000	III	2.6
23-03-2000	II	2.6
04-04-2000	Bd4	2.9
20-04-2000	Bd4	2.7
02-05-2000	Bd4	2.6
17-05-2000	Bd4	2.5
25-05-2000	Bd4	1.0
01-06-2000	Bd4	2.8
03-06-2000	I	3.2
06-06-2000	III	2.6
06-06-2000	II	2.6
21-06-2000	Bd4	1.9
03-07-2000	Bd4	3.2
11-07-2000	Bd4	1.4
17-07-2000	Bd4	2.3
01-08-2000	Bd4	3.3
16-08-2000	Bd4	2.5
28-08-2000	Bd4	2.9
01-09-2000	I	3.1
04-09-2000	III	1.7
04-09-2000	II	1.7
12-09-2000	Bd4	2.3
28-09-2000	II	3.3
28-09-2000	I	3.3
28-09-2000	Bd4	3.3
16-10-2000	Bd4	2.8
27-10-2000	II	3.0
27-10-2000	Bd4	3.0
06-11-2000	II	1.2
06-11-2000	Bd4	1.2
20-11-2000	Bd4	1.8
05-12-2000	Bd4	1.2
11-12-2000	II	3.0
11-12-2000	Bd4	3.0
08-01-2001	I	2.6
10-01-2001	III	3.1
10-01-2001	II	3.1
12-01-2001	Bd4	3.0

the stage above datum (m), M is the reciprocal Manning number ($m^{1/3} s^{-1}$), R is the hydraulic radius (m) and α is the momentum correction factor.

The bathymetric description of the Mondego's SA system was based on local maps. It is constituted by 17 cross-section profiles, a channel grid with 40 nodes, and four boundary points. The channel grid describes the riverbed configuration, and boundaries (Bd) give information about the system limits and flow type on each point. The "Bd1" – Pranto River sluice – was defined as a closed boundary with water discharges (manually controlled, depending on agricultural water needs). It means that at "Bd1" the water flows only forward to the sea, and only when sluice gates are open. The "Bd2" – the uppermost end of Armazéns channel – was defined as a closed boundary with a very weak and continuous water discharge of $0.002 m^3 s^{-1}$. The "Bd3" – the split point between north and south arms – was defined as an open boundary with no water discharge. The water was allowed to flow out of the boundary, with the same

volume returning into the system afterwards. Due to the small dimensions of the aperture the tide elevation is not imposed here as a forcing function, and the volume depends on the water level inside the system. Tides with higher amplitude allow a greater volume of water to cross outwards the boundary, returning inwards the same water volume on the next ebbing tide. The outer boundary "Bd4" – closest to the sea – was defined as an open boundary, influenced by tidal action, it is the exchange point and where the model is forced (Fig. 1). Changes on the water level impose inflow or outflow of water mass, reproducing the oscillatory movement of water observed on estuaries.

The HD module simulated water fluxes (Q) to the SA for a full year. It was based on the water conditions at "Bd1", "Bd2" and "Bd3", on the water level time-series that forced the system through "Bd4", and on the wind conditions that influenced the system on the water surface. Data on water discharged through the sluice were supported by field measurements of current velocities registered on a known channel section (Bd1), data on water levels came from Figueira da Foz harbour tide table (Bd4), and the information about the wind speed and wind direction was supplied by the Portuguese Navy (four measurements per day). The HD module was calibrated against the field water level measurements at sampling site II (Fig. 1).

The advection–dispersion (AD) module is based on the one-dimensional equation for conservation of mass of a dissolved compound. The sub-model requires output from the HD module, specified in time and space, in terms of discharge, water level, cross-sectional area and hydraulic radius. The advection–dispersion Eq. (3) is solved numerically by using an implicit finite difference scheme that has a negligible numerical dispersion, and reflects the advective transport and the dispersive transport due to the gradient concentration:

$$\frac{\partial AC}{\partial t} + \frac{\partial QC}{\partial x} - \frac{\partial}{\partial x} \left(AD \frac{\partial C}{\partial x} \right) = -AKC + C_s q \quad (3)$$

where A is the cross-sectional area (m^2), C is the concentration ($g m^{-3}$), t is the time coordinate (s), Q is the discharge ($m^3 s^{-1}$), x is the space coordinate (m), D is the dispersion coefficient ($m^2 s^{-1}$), K is the linear decay coefficient (s^{-1}), C_s is the source/sink concentration ($g m^{-3}$) and q is the lateral discharge ($m^2 s^{-1}$).

The advection–dispersion model was calibrated against field measurements of salinity due to its conservation properties.

The generated water flux (Q) was used to create the nutrients' mass flux in the system. Hourly average results of "Q" together with nutrient concentrations in water and filters were used to estimate the mass balance, respectively, of dissolved inorganic nitrogen and phosphorus ($DIN = NH_4-N + NO_3-N + NO_2-N$; $DIP = PO_4-P$), and of total nitrogen and phosphorus in suspended particulate matter (SPM-N and SPM-P).

Information about discrete residence time inside the system was obtained from AD simulations of a conservative substance (tracer). The total renewal of water is often difficult in estuaries, considerably increasing the residence time if this residual

volume is expected to completely leave the system (Braunschweig et al., 2003). To avoid excessively high residence time values, it was assumed that renewal was complete when the tracer fell to 5% of its initial concentration. Average values for consecutive periods of 12 h were considered, because the tracer can vary from 0% at low tide and above 5% at high tide in that time. The residence time was then estimated under different hydraulic conditions, varying from the minimal to maximal recorded discharge from the Pranto sluice (0.001, 10 and 28.45 m³ s⁻¹).

The water quality (WQ) module deals with basic aspects of river water quality in areas influenced by human activities (e.g. oxygen depletion and ammonia levels as a result of organic/nutrient loadings). The WQ module is coupled to the AD module, which means that the WQ module deals with chemical/biological transforming processes of multi-compound systems and the AD module is used to simulate the simultaneous transport process. The WQ module solves the system of coupled differential equations describing physical, chemical and biological interactions in the river (e.g. degradation of organic matter, photosynthesis and respiration of plants, and nitrification and exchange of oxygen with the atmosphere). The mass balance for involved parameters is calculated for all grid points at all time steps, using a rational extrapolation method in a two-step procedure integrated with the AD module.

The eutrophication (EU) module, available in the WQ module, is an advanced tool that describes the growth of phytoplankton, zooplankton, benthic vegetation and oxygen conditions as a consequence of BOD, nutrient availability and factors such as the incident light intensity, water temperature and the hydraulic conditions. The biological and chemical systems, described in the EU module, consist of a network of coupled processes where changes in one component can influence all the other variables, depending on the biological reaction involved. The 12 state variables included in the model are: chlorophyll concentration, phytoplankton carbon, phytoplankton nitrogen, phytoplankton phosphorus, zooplankton carbon, detritus carbon, detritus nitrogen, detritus phosphorus, dissolved inorganic nitrogen, dissolved inorganic phosphorus, dissolved oxygen and benthic vegetation carbon. The processes linked to these state variables considered in the model are: phytoplankton production, phytoplankton sedimentation, grazing, phytoplankton extinction, zooplankton excretion, zooplankton extinction, zooplankton respiration, mineralization of suspended detritus, sedimentation of detritus, mineralization of detritus, accumulation in sediment, benthic vegetation production, benthic vegetation extinction, and exchange with surrounding water (for further information see Flindt and Kamp-Nielsen, 1997).

2.4. Sensitivity tests and importance of biological components

Sensitivity tests were conducted to evaluate the importance of different biological factors to the model and to all the processes occurring in the system. The values of some crucial parameters (e.g. the growth rates, production temperature

dependency, N and P uptake rates, grazing and sedimentation rates, relative to the phytoplankton and macroalgae) were changed by 10% (up and down), and the obtained results simply correlated with the ones from the normal simulation. This way it was possible to evaluate the variations induced by the main biological processes to the concentration of several nutrient forms (e.g. dissolved fraction, adsorbed to particulate matter, or included in phytoplankton or macroalgae), and to dissolved oxygen values.

When the WQ and EU modules are running, the dissolved oxygen in the system must be within measured levels, so that the simulation of environmental processes is properly performed, balanced between autotrophic production and oxygen consumption in heterotrophic processes.

To evaluate the importance of the total biological processes for the SA system, a simulation was performed without the WQ and EU modules. Only the HD and AD modules were used for this purpose. The difference should give an idea of the magnitude of the biological and physico-chemical processes in relation to the estuarine system.

3. Results

3.1. Calibration and validation

For the Mondego Estuary a full year's run was performed. The evolution of the water level at Bd4 during this period followed a semi-diurnal pattern (two high tides and two low tides per day), with tidal range from 0.25 m to 3.67 m as extreme registered values. As a calibration point in the system it was decided to use sampling site II (Fig. 1), the Pranto River (immediately upstream of the junction with SA), because this is far enough inside the system (3 km upstream of the exchange boundary Bd4) and it also captures the influence of that tributary (important nutrient source for the SA).

The values of the basic calibration parameters used in the model, and the correlation values found between simulation results and field measurements at calibration point (II) can be seen in Table 2. The good results obtained demonstrate the individual functioning of HD, AD, WQ and EU modules, and their globally good integration into the SA simulation.

Concerning the advection–dispersion (AD) sub-model, it is clear that simulated values for salinity (conservative element) fitted well with field measurements made at calibration point II, which constitutes a positive indication for the AD module's functioning. Dissolved oxygen was never depleted or oversaturated in the simulation, suggesting a balanced relation between oxygen production and oxygen consumption processes inside the system. Although oxygen correlations were not very strong, basically because some of the processes responsible for its production and consumption were kept absent to maintain the model's simplicity, one can agree on the correct functioning of the water quality (WQ) sub-model. The good calibration of the eutrophication module demonstrates the correct functioning of the network of biological and chemical coupled processes comprising the module. The correlation values found between

Table 2
Basic calibration values used in the model and correlations found between simulation results and parameters measured at sampling site II

Module	Parameter	Constant/rate	Basic calibration value	Unit
HD	Bed resistance	Manning (M)	50	m ^{1/3} s ⁻¹
AD	Dispersion	Dispersion factor Exponent	10 1	Disp (m ² s ⁻¹)
WQ	Benthic vegetation	Benthic slouching rate	0.015	day ⁻¹ at 20 °C
		Production rate of benthic vegetation	0.04	day ⁻¹ at 20 °C
	Detritus	Detritus C mineralization rate at 20 °C	0.05	day ⁻¹ at 20 °C
		Sedimentation rate, for depth < 2 m	0.06	day ⁻¹ at 20 °C
		Sedimentation rate, for depth > 2 m	0.06	day ⁻¹ at 20 °C
	Light extinction	Light extinction constant for phytoplankton	20	m ⁻¹
		Light extinction constant for detritus	0.3	m ⁻¹
		Light extinction background constant range	0.2	m ⁻¹
		Light extinction constant for benthic vegetation	1	m ⁻¹
	Oxygen	Reaeration constant for dissolved oxygen	1.5	day ⁻¹ at 20 °C
	Phytoplankton	Maximum growth rate for diatoms at 5 °C	1	day ⁻¹ at 5 °C
		Maximum growth rate for green algae at 20 °C	1.1	day ⁻¹ at 20 °C
		Phytoplankton sedimentation rate, for depth < 2 m	0.3	day ⁻¹ at 20 °C
		Phytoplankton sedimentation rate, for depth > 2 m	0.3	day ⁻¹ at 20 °C
		Maximum grazing rate at 20 °C	1	day ⁻¹ at 20 °C
		Maximum death rate for starving phytoplankton	0.06	day ⁻¹ at 20 °C
	Sediment	Proportion factor for N release from sediment	1.1	day ⁻¹ at 20 °C
		Proportion factor for P release from sediment	1.5	day ⁻¹ at 20 °C
		Proportion factor for sediment respiration	1.75	day ⁻¹ at 20 °C
	Zooplankton	Death rate constant (m ³ /g/day)	7.5	day ⁻¹ at 20 °C
Death rate constant (/day)		0.07	day ⁻¹ at 20 °C	
		Correlation simulation/measured	<i>n</i>	
	Salinity	0.98	56	
	Oxygen	0.44	40	
	DIN	0.67	71	
	DIP	0.25	56	
	Chl <i>a</i>	0.62	43	
	SPM-N	0.43	43	
	SPM-P	0.66	31	

the measured and simulated concentrations of nutrients (dissolved and adsorbed to SPM) suggest that the transport in the water column is simulated well by the model. The weakest correlations observed to DIP and SPM-N are strongly influenced by the P-mineralization occurred during warmer periods, and by the over simulation of SPM-N during some parts of the year. These processes still need further attention; the inclusion of other biological elements (e.g. salt marshes) and sources (e.g. fish farms), and the distinction between SPM with different quality contents in different seasons surely will contribute to future simulation result's improvement. Fig. 2 shows field measurements and simulation results for some elements; salinity (Fig. 2A), as an important element for testing the AD sub-module efficiency; oxygen (Fig. 2B), to evaluate the output range of simulation results from the WQ sub-module; and dissolved nutrients (Fig. 2C) and nutrients adsorbed to suspended particulate matter (Fig. 2D) to show the performance achieved by coupled AD and WQ sub-modules.

The simulation of benthic biomass relates to macroalgal production. The simulation peaks were of the same range as

values of benthic biomass production in the field, although they were achieved 2 months later in time.

3.2. Water and nutrient mass balance

The hydrologic balance was 1,300,000 m³, the difference between the annual water input from sluice at Bd1 (“*Q*” import), and the output through the outer boundary at Bd4 (“*Q*” export). The values are presented as monthly accumulated volumes, and of the annual “*Q*” import of 44,500,000 m³, there was a poor contribution from June to November (20%), in contrast to the wettest period of the year which contributed up to 80% to the total water balance (January to May and December).

The sluice discharge is very dependent on precipitation, and a high correlation was found between accumulated water flux inputs and accumulated precipitation (Fig. 3). The delay observed in the release of fresh water from the fields during low precipitation periods (part of spring and summer) is due to the dependency of sluice operations on the water needs of

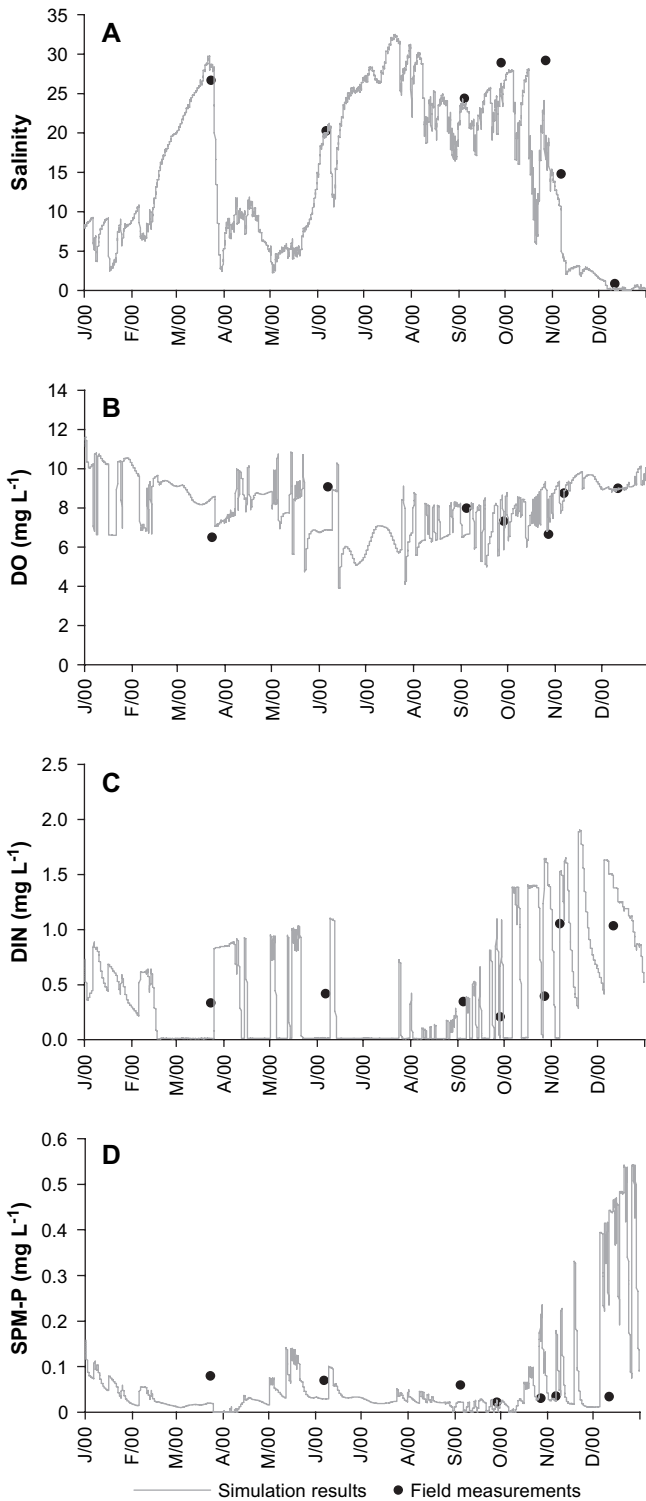


Fig. 2. Field measurements vs. simulation results for salinity (A), dissolved oxygen (B), dissolved inorganic nitrogen (C) and phosphorus adsorbed to suspended particulate matter (D), at sampling site II.

the farmland. The water is deliberately stored during this period to be used on the rice fields.

Residence times estimated with sluice discharges of 0.001, 10.0 and 28.45 m³ s⁻¹ were, respectively, 5.4, 1.9 and 1.3 days for the Bd4, and 14.8, 1.1 and 1.1 days inside the system

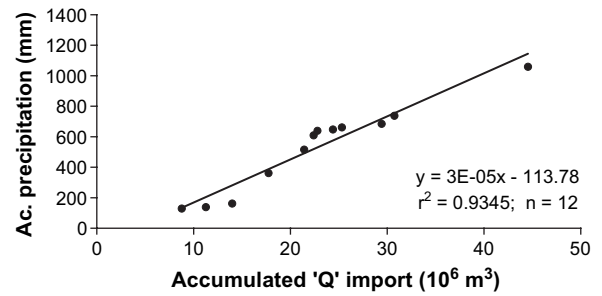


Fig. 3. Correlation found between accumulated water flux at the sluice ('Q' import) and monthly-accumulated precipitation.

(Pranto River) (Fig. 4). The tracer peaks (higher than 5%) observed after the calculated residence time for both sites occurred during the flood periods, when the remaining water (which did not leave the system) was pushed upstream by the incoming marine water.

The drifting vegetation collected led to the calculation that green macroalgae constituted 36% of the total biomass export in winter, 58% in spring, 37% in summer and 14% in the autumn. It was estimated that around 12% of standing biomass of green macroalgae was drifted out of the system each month. A significant correlation was found between standing biomass and transported biomass ($y = 0.0965x - 1209.1$; $R^2 = 0.8323$). It was assumed, based on the previous calculation, that macroalgae present at a given moment were available for subsequent transportation, so the available macroalgae and the macroalgae transported a time step later were correlated. The late summer period was not considered here due to its high export values. The biomass export reached up to 30% of the standing biomass when the system is fluxed by sluice discharges that occur before and after the crop season.

Different nutrient fractions (dissolved inorganic, adsorbed to suspended particulate matter or bound in vegetation) were calculated as monthly accumulated values (Table 3). All nutrient forms had low import values at Bd1 in summer (July–September), when the sluice was closed. At Bd4, both import and export situations were observed, and a particular seasonal dynamics characterised each nutrient fraction at this boundary.

Concerning dissolved nutrients, DIN export was high in January, April, November and December, when the sluice was open. DIN import occurred through Bd4 from May to September (negative export), when the sluice was closed. DIP export was higher during the summer and in December.

Nutrients adsorbed to suspended particulate matter behave differently from the dissolved fraction. SPM-N export was always positive with the higher values reached in June, and SPM-P was positive only in January, May, June and December. The Veg-N and Veg-P export were high in January, February, May and July, and an import was actually seen to occur through this boundary for most of the rest of the year (Table 3).

With respect to annual dynamics, nitrogen import was dominated in 92% by the dissolved fraction (46 t N), but export, on the other hand, was dominated in 85% by the fraction adsorbed to suspended particulate matter (39 t N). The Veg-N export through Bd4 represented 5% of total export and reached 2 t

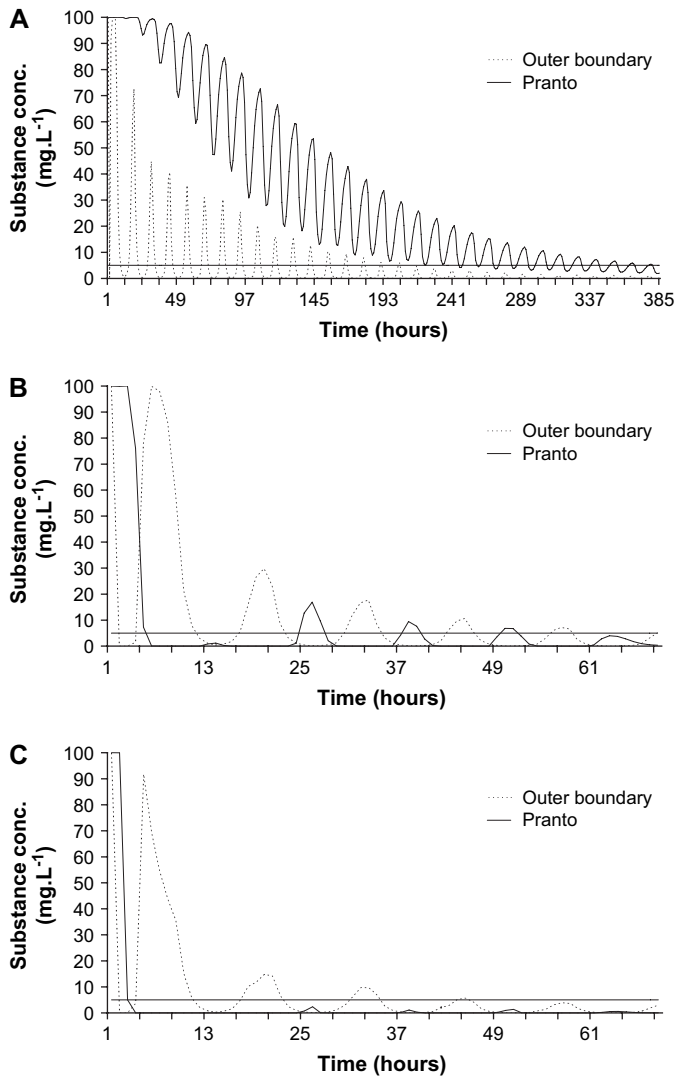


Fig. 4. Estimations of residence time under different hydraulic conditions at the outer boundary and at the Pranto River mid-point. The longer residence time was simulated under nearly no sluice discharge, $0.001 \text{ m}^3 \text{ s}^{-1}$ (A), the mean residence time was simulated under a discharge of $10 \text{ m}^3 \text{ s}^{-1}$ (B), and the shortest residence time was simulated under a water discharge of $28.45 \text{ m}^3 \text{ s}^{-1}$ (C).

N. Phosphorus import occurred 85% under the SPM-P fraction (9 t P through the sluice and 3 t P at Bd4), and export was dominated in 99.7% by DIP (28 t P). Veg-P contributed with 0.3% to the total P export (88 kg P) from the SA through the Bd4.

The annual nitrogen mass balance was 3.6 t N retained inside the system, the difference between 50 t N import and 46 t N export. The annual phosphorus balance was 14 t P leaving the system (Table 3).

3.3. Sensitivity tests and importance of biological components

Results from the simulation based on HD and AD modules alone showed that some nutrient forms can be strongly influenced by biological activity, which discards the mimic effect from Bd4 that alone could be expected to rule the simulation

results (Table 4). Dissolved oxygen and DIP varied considerably, but not SPM-P and DIN, which showed higher correlations between the results obtained with the complete simulation (including water quality and eutrophication modules) and the one excluding biological components (only the HD and AD modules).

In Table 4, the sensitivity analysis shows the correlation values obtained for normal simulation vs. simulations using a rate 10% less (to several components), correlation obtained for normal simulation vs. simulations using a rate 10% more (for several components), and the correlation values between simulations using rates both 10% less and more. Sensitivity analysis always showed a lower correlation for benthic macroalgal production (BC), and in contrast, high correlations for the SPM-P. Nutrients included in phytoplankton were more affected by phytoplankton maximal growth rate; nutrients adsorbed to SPM were more affected when the macrophyte light extinction rate was modified; nutrients' dissolved fractions were more affected by changes in macrophyte maximal growth rate; and the phytoplankton had great influence on the production of benthic macroalgae.

4. Discussion

The high correlation found between accumulated fluxes at Bd1 “Q” (input) and precipitation suggested a cascade of influences, where precipitation influenced water availability, which influenced field water needs that eventually influenced the sluice discharge. This confirms the previous idea of the high dependency of sluice management on agricultural water needs (Lillebø et al., 1999; Pardal et al., 2000; Martins et al., 2001; Cardoso et al., 2002; Dolbeth et al., 2003). The water discharges, given the high volumes usually involved, force salinity levels to fall and supply nutrients to the SA as increased freshwater inputs through Bd1.

DIN fraction dominated 92% of total nitrogen loading through the sluice, pinpointing farmland as the major source of nitrogen for the SA. The results obtained by simulation, with and without the biological elements (Table 4), suggest that N import was more than sufficient to support the primary production needs of the system. Moreover, DIN import also occurred through Bd4 when the sluice was closed (probably related to summer tourism and other diverse sources such as fish farms). This indicates a great N-retention capacity of the system during the summer period. DIN concentration decreased inside the system; supposedly it was incorporated into primary producers that left the system as suspended particulate matter (SPM-N). This was supported by low SPM-N import (8% of total N import) and its high export value (85% of total N export) mainly during the warmer period. This fact can be easily ascribed to fragmentation and/or decomposition of primary producers. DIN export was less important, at 10% of its total amount.

Phosphorus bound to suspended particulate matter (SPM-P) dominated the import (85% of total P import). As stated above in relation to DIN, the comparison between results for SPM-P from the simulations with and without biological processes

Table 3
Monthly import and export dynamics, and annual import, export and mass balance of different nitrogen and phosphorus fractions (N and P kg)

	Import (kg)			Export (kg)		
	DIN	SPM-N	Veg-N	DIN	SPM-N	Veg-N
Jan-2000	6069	175	0	9576	4606	488
Feb-2000	1626	58	0	1600	841	520
Mar-2000	2329	124	0	1599	666	-3
Apr-2000	3403	200	0	7884	1764	-333
May-2000	3709	433	0	-25,408	9819	599
Jun-2000	1103	84	0	-14,113	10,137	-64
Jul-2000	234	28	0	-7960	3431	1508
Aug-2000	302	47	0	-4104	1384	-37
Sep-2000	694	57	0	-1713	1294	-23
Oct-2000	6072	431	0	4924	470	37
Nov-2000	2349	224	0	8556	1505	-616
Dec-2000	17,892	2138	0	23,896	3350	88
Sub-total	45,782	4000	0	4736	39,267	2165
Total			49,782			46,168
Nitrogen mass balance (export–import)						-3614
	DIP	SPM-P	Veg-P	DIP	SPM-P	Veg-P
Jan-2000	198	679	0	2045	229	38
Feb-2000	56	143	0	1718	-1339	40
Mar-2000	49	8	0	2374	-2185	5
Apr-2000	58	23	0	1042	-1756	-8
May-2000	186	454	0	-851	265	19
Jun-2000	78	113	0	1272	1360	0
Jul-2000	76	30	0	3010	-551	7
Aug-2000	32	52	0	4069	-2527	-1
Sep-2000	41	7	0	3130	-954	-7
Oct-2000	85	411	0	1856	-267	2
Nov-2000	67	327	0	1789	-72	-20
Dec-2000	1193	6555	0	6758	4694	4
Sub-total	2119	8803	0	28,213	-3104	80
Total			10,922			25,188
Phosphorus mass balance (export–import)						14,267

(high correlation values) also suggests a high input of this P fraction into the system that not biologically consumed afterwards. Upstream areas (e.g. agriculture fields) were a great P-source for the SA. SPM-P increased during sluice-opening periods in April–May and the winter. On the other hand, DIP was mainly generated inside the system during warmer periods (Flindt et al., 1997; Touchette and Burkholder, 2000; Lillebø et al., 2002). SPM-P was retained inside the system and later, after mineralization and efflux to the water column, phosphorus was exported as DIP to adjacent areas (Grenz et al., 2000; Mortazavi et al., 2000b; Nielsen et al., 2001).

Although the external nutrient loading has fallen in many estuaries, they are only beginning to adjust to this change, and several of them still show high internal nutrient loadings. This excess of nutrients, helped by favourable hydrodynamic conditions, may trigger opportunist primary producer growth, a process by which the incorporated nutrients are transformed into a different fraction. In productive shallow estuaries the incorporated nutrients may represent a considerable part of the total pool of nutrients in the system. If this fraction is not included in the mass balance evaluations an equally large miscalculation can be made. However, it seems that

the plant-bound nutrient transport is less essential to the nutrient mass balance in macro-tidal systems, where production is diminished due to high turbidity and hydrodynamic forces. Even though important primary production may occur in different seasons, or when environmental conditions change (e.g. engineering works, hydromorphological modification), increasing the importance of its inclusion in mass balance for almost all systems.

In relation to the Mondego Estuary's SA, the vegetation export had a small relative importance for the total mass balance in 2000; it represented 5% of total N export and 0.5% of P export. But a completely different scenario occurred when macroalgal blooms were observed at the system, and the transport of vegetation became more important for nutrient mass balance. Comparing data from 1993 and 2000, green macroalgae reached in 1993 a biomass more than three times higher than for 2000, and biomass export was four times greater than the value of 2000. If similar mass balance conditions to 1993 were considered, Veg-N export could represent up to 20% of total N export of the system and Veg-P export about 1.5% of total P export. In these circumstances nutrient dynamics could be quite different. The increase of nutrients required by green macroalgae would make the dissolved fraction export considerably lower than that calculated for 2000, thereby increasing the relative importance of the bound to vegetation fraction. This result reinforces the importance of including vegetation in mass balance studies, otherwise a significant part of nutrient mass is missed.

Salomonsen et al. (1999) reported for Møllekrogen, a sub-system of the micro-tidal Roskilde Fjord (Denmark), Veg-N export of 35% of total N export and Veg-P export of 81% to total P export during the summer, and Flindt et al. (1997) estimated for the Venice Lagoon meso-tidal system a Veg-N export of 95% of total N export and Veg-P of 91% to total P export in the growth season. Comparing the three systems, it seems that tidal amplitude is not a critical aspect in the relative importance of vegetation for the total nutrient export. It is much more a question of environmental conditions, in particular plant production, absolute water nutrient concentrations coupled with hydrodynamics, since higher residence times allow longer availability of nutrients for primary producer consumption (Mortazavi et al., 2000a; Nielsen et al., 2001).

5. Conclusions

As a general conclusion we may say that the system is still not balanced and the over-loaded sediments may now be working as a nutrient source. For a better environmental situation, nutrient inputs and residence time in the system should be lower. The latter can be achieved by enlarging the channel at the splitting point between the arms (Bd3 – Fig. 1), and the former by reducing nutrient losses from arable land which get into the system through the Pranto River sluice. The nutrient input reduction could be accomplished in two main ways: (1) source management (e.g. better use of fertilisers); and (2) transport management (e.g. water flow through wetlands and

Table 4

Results from sensitivity tests. Correlation values between normal simulations and simulations where it was increased (+) or decreased (–) the rate values for each indicated factor. Correlation values between simulations where the rate values were increased and where the rate values were decreased for each factor considered (+/–). Correlation between normal simulation and the simulation running only with hydrodynamic (HD) and advection–dispersion (AD) modules turned on (no biological elements considered)

Correlations	Phyto-C	Phyto-N	Phyto-P	Chl <i>a</i>	SPM-C	SPM-N	SPM-P	DIN	DIP	DO	Veg-C
Phyto max growth rate (+)	0.916	0.884	0.921	0.871	0.913	0.882	0.991	0.947	0.853	0.958	0.676
Phyto max growth rate (–)	0.990	0.987	0.990	0.982	0.996	0.995	0.999	0.982	0.852	0.990	0.780
Phyto max growth rate (+/–)	0.749	0.772	0.738	0.939	–0.190	–0.142	0.004	0.229	–0.354	0.961	0.018
Phyto sedimentation rate (+)	0.978	0.970	0.979	0.965	0.986	0.984	0.998	0.976	0.877	0.990	0.777
Phyto sedimentation rate (–)	0.931	0.906	0.935	0.889	0.924	0.900	0.992	0.957	0.849	0.961	0.688
Phyto sedimentation rate (+/–)	0.756	0.795	0.744	0.994	–0.124	–0.061	0.028	0.219	–0.366	0.998	0.089
Phyto grazing rate (+)	0.958	0.941	0.960	0.932	0.957	0.948	0.995	0.969	0.864	0.977	0.740
Phyto grazing rate (–)	0.958	0.941	0.959	0.932	0.956	0.947	0.995	0.969	0.864	0.976	0.739
Phyto grazing rate (+/–)	0.752	0.786	0.740	0.975	–0.177	–0.124	0.009	0.233	–0.355	0.986	0.057
Phyto N uptake/N available (+)	0.958	0.942	0.960	0.932	0.956	0.947	0.995	0.969	0.864	0.976	0.740
Phyto N uptake/N available (–)	0.957	0.941	0.959	0.932	0.958	0.949	0.995	0.969	0.864	0.977	0.740
Phyto N uptake/N available (+/–)	0.751	0.786	0.739	0.975	–0.178	–0.125	0.009	0.233	–0.355	0.985	0.057
Phyto P uptake/P available (+)	0.958	0.941	0.959	0.932	0.957	0.948	0.995	0.969	0.864	0.976	0.740
Phyto P uptake/P available (–)	0.958	0.941	0.960	0.932	0.957	0.948	0.995	0.969	0.864	0.977	0.740
Phyto P uptake/P available (+/–)	0.752	0.786	0.740	0.975	–0.178	–0.125	0.009	0.233	–0.355	0.985	0.057
Macro max growth rate (+)	0.960	0.944	0.962	0.933	0.978	0.974	0.998	0.970	0.869	0.985	0.807
Macro max growth rate (–)	0.954	0.939	0.955	0.932	0.921	0.900	0.978	0.967	0.858	0.964	0.655
Macro max growth rate (+/–)	0.750	0.786	0.739	0.975	–0.142	–0.078	0.022	0.213	–0.371	0.995	0.089
Macro light extinction const (+)	0.944	0.925	0.947	0.913	0.942	0.928	0.994	0.965	0.861	0.972	0.724
Macro light extinction const (–)	0.944	0.925	0.947	0.913	0.942	0.928	0.994	0.965	0.861	0.972	0.724
Macro light extinction const (+/–)	0.753	0.783	0.741	0.965	–0.203	–0.169	–0.005	0.233	–0.351	0.980	0.046
Macro N uptake (+)	0.956	0.940	0.957	0.932	0.938	0.923	0.993	0.968	0.861	0.970	0.692
Macro N uptake (–)	0.959	0.943	0.961	0.932	0.972	0.967	0.997	0.970	0.868	0.982	0.782
Macro N uptake (+/–)	0.754	0.787	0.742	0.974	–0.191	–0.144	0.005	0.244	–0.346	0.976	0.040
Macro respiration rate (+)	0.956	0.940	0.958	0.932	0.936	0.921	0.993	0.968	0.860	0.970	0.689
Macro respiration rate (–)	0.959	0.942	0.961	0.932	0.973	0.968	0.997	0.970	0.868	0.982	0.784
Macro respiration rate (+/–)	0.754	0.787	0.742	0.974	–0.193	–0.147	0.004	0.244	–0.345	0.975	0.037
HD + AD modules	0.345	0.419	0.328	0.797	0.335	0.388	0.584	0.455	0.191	0.054	

salt marshes, restored or constructed, using their potential to remove N and P from water column).

As stated above, the south arm of the Mondego Estuary is still exporting nutrients as a result of decades of retention due to anthropogenic activities. If eroded, the enriched sediments may be a great source of phosphate, so sluice discharge should be smoothed to avoid re-suspension. It is preferable to have shorter opening periods although they could occur more often.

Dissolved inorganic and adsorbed to SPM fractions dominated the nutrient mass balance in this meso-tidal system but the fractions bound in vegetation can also perform a very important role, mainly when macroalgal blooms occur. It seems that tidal amplitude was not a crucial aspect governing the vegetation's relative importance for total nutrient export but the environmental conditions supporting its growth were. The importance of plant-bound nutrient transport was quite different, depending on the different eutrophic scenarios of the system (with or without macroalgal blooms).

The simulation accuracy was quite satisfactory, opening the possibility for the model's use as a management tool for the SA. Different nutrient fractions (concentrations) can be calculated for several scenarios (e.g. reference conditions under the WFD). Moreover, the results achieved showed us the model can perform well with the biological elements and internal dynamics of the system, not mimicking the conditions imposed at the outer boundary.

Acknowledgements

This study was carried out under the POCTI – Formar e Qualificar – Medida 1.1 program (Portuguese FCT) through a PhD grant to João Magalhães Neto (Praxis XXI/BD/18422/98).

References

- APHA (American Public Health Association), 1980. Standard Methods for the Examination of Water and Wastewater, 15th ed. APHA, Washington, D.C., 1134 pp.
- Beetink, W.K., 1977. The coastal salt marshes of western and northern Europe: an ecological and phytosociological approach. In: Chapman, V.J. (Ed.), Wet Coastal Ecosystems. Elsevier, Amsterdam, pp. 109–155.
- Bouchard, V., Lefeuvre, J.C., 2000. Primary production and macro-detritus dynamics in a European salt marsh: carbon and nitrogen budgets. *Aquatic Botany* 67, 23–42.
- Braunschweig, F., Martins, F., Chambel, P., Neves, R., 2003. A methodology to estimate renewal time scales in estuaries: the Tagus Estuary case. *Ocean Dynamics* 53, 137–145.
- Cardoso, P.G., Lillebø, A.I., Pardal, M.A., Ferreira, S.M., Marques, J.C., 2002. The effect of different primary producers on *Hydrobia ulvae* population dynamics: a case study in a temperate intertidal estuary. *Journal of Experimental Marine Biology and Ecology* 277, 173–195.
- Cardoso, P.G., Pardal, M.A., Lillebø, A.I., Ferreira, S.M., Raffaelli, D., Marques, J.C., 2004. Dynamic changes in seagrass assemblages under eutrophication and implications for recovery. *Journal of Experimental Marine Biology and Ecology* 302, 233–248.

- Diaz, R.J., Rosenberg, R., 1995. Marine benthic hypoxia: a review of its ecological effects and the behavioural responses of benthic macrofauna. *Oceanography and Marine Biology: An Annual Review* 33, 245–303.
- Dolbeth, M., Pardal, M.A., Lillebø, A.I., Azeiteiro, U., Marques, J.C., 2003. Short- and long-term effects of eutrophication on the secondary production of an intertidal macrobenthic community. *Marine Biology* 143, 1229–1238.
- Duarte, C.M., 2000. Marine biodiversity and ecosystem services. *Journal of Experimental Marine Biology and Ecology* 250, 117–132.
- Flindt, M.R., Kamp-Nielsen, L., 1997. Modelling of an estuarine eutrophication gradient. *Ecological Modelling* 102, 143–153.
- Flindt, M.R., Kamp-Nielsen, L., Marques, J.C., Pardal, M.A., Bocci, M., Bendoricchio, G., Salomonsen, J., Nielsen, S.N., Jørgensen, S.E., 1997. Description of the three shallow estuaries: Mondego River (Portugal), Roskilde Fjord (Denmark), and the Lagoon of Venice (Italy). *Ecological Modelling* 102, 17–31.
- Flindt, M.R., Pardal, M.A., Lillebø, A.I., Martins, I., Marques, J.C., 1999. Nutrient cycling and plant dynamics in estuaries: a brief review. *Acta Oecologica* 20, 237–249.
- Flindt, M.R., Neto, J., Amos, C.L., Pardal, M.A., Bergamasco, A., Pedersen, C.B., Andersen, F.Ø., 2004. Plant bound nutrient transport. Mass transport in estuaries and lagoons. In: Nielsen, S.L., Banta, G.T., Pedersen, M.F. (Eds.), *Estuarine Nutrient Cycling: The Influence of Primary Producers. The Fate of Nutrient Biomass. Series: Aquatic Ecology*, vol. 2, pp. 93–128.
- Grenz, C., Cloern, J.E., Hager, S.W., Cole, B.E., 2000. Dynamics of nutrient cycling and related benthic nutrient and oxygen fluxes during a spring phytoplankton bloom in South San Francisco Bay (USA). *Marine Ecology Progress Series* 197, 67–80.
- Hemminga, M.A., Cattrijsse, A., Wielemaker, A., 1996. Bedload and nearbed detritus transport in a tidal saltmarsh creek. *Estuarine, Coastal and Shelf Science* 42, 55–62.
- Hobbs, R.J., Norton, D.A., 1996. Towards a conceptual framework for restoration ecology. *Restoration Ecology* 4, 93–110.
- de Jonge, V.N., de Jong, D.J., van Katwijk, M.M., 2000. Policy plans and management measures to restore eelgrass (*Zostera marina* L.) in the Dutch Wadden Sea. *Helgoland Marine Research* 54, 151–158.
- Kronvang, B., Svendsen, L.M., Jensen, J.P., Dørge, J., 1999. Scenario analysis of nutrient management at the river basin scale. *Hydrobiologia* 410, 207–212.
- Lefevre, J.C., 1994. Comparative studies on salt marsh processes in the baie du Mont Saint-Michel: a multi-disciplinary study. In: Mitsch, W.J. (Ed.), *Global Wetlands: Old World and New*. Elsevier, Amsterdam, pp. 215–234.
- Lillebø, A.I., Pardal, M.A., Marques, J.C., 1999. Population structure, dynamics and production of *Hydrobia ulvae* (Pennant) (Mollusca: Prosobranchia) along an eutrophication gradient in the Mondego Estuary (Portugal). *Acta Oecologica* 20, 289–304.
- Lillebø, A.I., Flindt, M.R., Pardal, M.A., Martins, I., Neto, J.M., Marques, J.C., 2002. Nutrient dynamics in the intertidal pools of the Mondego Estuary. II – seasonal efflux of PO₄-P and NH₄-N in bare bottom and vegetated pools. In: Pardal, M.A., Marques, J.C., Graça, M.A.S. (Eds.), *Aquatic Ecology of the Mondego River Basin. Global Importance of Local Experience*. Imprensa da Universidade de Coimbra, pp. 257–271.
- Limnologisk Metodik, 1992. Ferskvandsbiologisk Laboratorium. Københavns Universitet (Ed.), Akademisk Forlag, København, 172 pp.
- Marques, J.C., Rodrigues, L.B., Nogueira, A.J.A., 1993. Intertidal macrobenthic communities structure in the Mondego Estuary (western Portugal): reference situation. *Vie et Milieu* 43, 177–187.
- Martins, I., Oliveira, J.M., Flindt, M.R., Marques, J.C., 1999. The effect of salinity on the growth rate of the macroalgae *Enteromorpha intestinalis* (Chlorophyta) in the Mondego Estuary (west Portugal). *Acta Oecologica* 20, 259–265.
- Martins, I., Pardal, M.A., Lillebø, A.I., Flindt, M.R., Marques, J.C., 2001. Hydrodynamics as a major factor controlling the occurrence of green macroalgae blooms in a eutrophic estuary: a case study on the influence of precipitation and river management. *Estuarine, Coastal and Shelf Sciences* 52, 165–177.
- Mortazavi, B., Iverson, R.L., Huang, W., Lewis, F.G., Caffrey, J.M., 2000a. Nitrogen budgets of Apalachicola Bay, a bar-built estuary in the northeastern Gulf of Mexico. *Marine Ecology Progress Series* 195, 1–14.
- Mortazavi, B., Iverson, R.L., Landing, W.M., Huang, W.R., 2000b. Phosphorus budget of Apalachicola Bay: a river-dominated estuary in the northeastern Gulf of Mexico. *Marine Ecology Progress Series* 198, 33–42.
- Nielsen, K., Risgaard-Petersen, N., Sømod, B., Rygaard, S., Bergø, T., 2001. Nitrogen and phosphorus retention estimated independently by flux measurements and dynamic modelling in the estuary, Randers Fjord, Denmark. *Marine Ecology Progress Series* 219, 25–40.
- Norkko, A., Bonsdorff, E., 1996. Population responses of coastal zoobenthos to stress induced by drifting algal mats. *Marine Ecology Progress Series* 140, 141–151.
- Pardal, M.A., Marques, J.C., Metelo, I., Lillebø, A.I., Flindt, M.R., 2000. Impact of eutrophication on the life cycle, population dynamics and production of *Ampithoe valida* (Amphipoda) along an estuarine spatial gradient (Mondego Estuary, Portugal). *Marine Ecology Progress Series* 196, 207–219.
- Pardal, M.A., Cardoso, P.G., Sousa, J.P., Marques, J.C., 2004. Assessing environmental quality: a novel approach. *Marine Ecology Progress Series* 267, 1–8.
- Raffaelli, D.G., Raven, J.A., Poole, L.J., 1998. Ecological impact of green macroalgal blooms. *Oceanography and Marine Biology: An Annual Review* 36, 97–125.
- Salomonsen, J., Flindt, M., Geertz-Hansen, O., Johansen, C., 1999. Modelling advective transport of *Ulva lactuca* (L.) in the sheltered bay, Mollekrogen, Roskilde Fjord, Denmark. *Hydrobiologia* 397, 241–252.
- Sfriso, A., Birkemeyer, T., Ghetti, P.F., 2001. Benthic macrofauna changes in areas of Venice Lagoon populated by seagrasses or seaweeds. *Marine Environmental Research* 52, 323–349.
- Strickland, J.D.H., Parsons, T.R., 1972. A practical handbook of seawater analysis. Pigment analysis. *Bulletin Fishery Research Board Canada*, 167–311.
- Touchette, B.W., Burkholder, J.M., 2000. Review of nitrogen and phosphorus metabolism in seagrasses. *Journal of Experimental Marine Biology and Ecology* 250, 133–167.
- Valiela, I., McClelland, J., Hauxwell, J., Behr, P., 1997. Macroalgal blooms in shallow estuaries: controls and ecophysiological and ecosystem consequences. *Limnology and Oceanography* 42, 1105–1118.
- World Health Organization, 2002. *Water – Eutrophication and Health*. European Commission, Luxembourg, 28 pp.